

Preparation and Identification of Some Graphene Oxide Derivatives Prepared From Graphite Straw of the Iraqi Wheat Crop

Budoor Khudair Hamad Al-Issawi, Ghazwan Hassan Abdul Wahab Al-Sumaidaie

Tikrit University/ College of Education for Pure Sciences/ Department of Chemistry

Abstract: In this research, the aromatic reduced graphene oxide derivative (B4:Ar-RGO) was prepared electrochemically using an electrochemical cell as an environmentally friendly method, by preparing diazonium salts of 4-amino benzoic acid in an acidic solution with reduced graphene oxide for straw from the Iraqi wheat crop, with a good yield and area. Excellent surface area, 1229 m²/g, with low grain size. Thiocarbohydrazide (TCH), prepared by reacting carbon disulphide with aqueous hydrazine(80%) , was used to prepare triazole for reduced graphene oxide (B5) by treating (B4:Ar-RGO) with thiocarbohydrazide by thermal melting without the need to use a solvent and with a good product ratio, and to prepare azo benzoic acid - Reduced graphene oxide (B6) from (B3:TSRGO) treatment with the diazonium salt of 4-amino benzoic acid with a good yield. As well as the preparation of triazole Schiff bases (B7) and (B8) by reacting (B5) with benzaldehyde and 2-hydroxybenzaldehyde, respectively, with a good product ratio, and B7 was the highest particle size among them.

Keywords: wheat straw, Reduce grapheme oxide, Schiff base, Triazoles

1. Introduction

Reduced graphene oxide consists of a single thin layer of graphene oxide, which is partially deoxygenated. Graphene oxide contains a number of functional groups such as oxygen and epoxy groups in addition to carboxyl groups, where oxygen is reduced by chemical reduction using strong reducing agents ⁽¹⁾ such as ammonia and hydroquinone. , as well as hydrazine hydrate ⁽²⁾

Triazoles are compounds with a heterogeneous pentagonal ring, containing two carbon atoms and three nitrogen atoms as part of their aromatic ring ⁽³⁾. They are weak bases that possess high stability and contain two isomers (3,2,1-triazole) (4,2,1-triazole). As in the formula below ⁽⁴⁾.



Laboratory-prepared triazole derivatives have been used to obtain many antibiotics, drugs, and dyes ⁽⁵⁾. Carboxylic acid substitutes have been used in the preparation of triazole, which has medical importance, including as anti-cancer agents ⁽⁶⁾.

Schiff bases consist of the condensation of amines with ketones or aldehydes. They were named after the scientist (Hugo Schiff), who prepared these compounds for the first time in 1864AD ⁽⁷⁾. They are also called by other names depending on the method of their preparation, such as the azomethine group (C = N). Which contains an imine group ⁽⁸⁾, and the imine compound is crystalline and disintegrates quickly ⁽⁹⁾, so it contains at least one aryl group substituted on a carbon or nitrogen atom to increase the stability of the compounds, as it was found that the stability of these compounds depends on the type of amines, aldehydes, and ketones used ⁽¹⁰⁾.

2. Experimental details

2.1. Preparation of thiocarbohydrazide (TCH)

Place 5ml of carbon disulphide in a 100ml round flask in an ice bath, then add 20ml of aqueous hydrazine (80%) dropwise over 10minutes with continuous stirring, then rise the mixture for 30minutes, collect the precipitate (yellow colour). By filtration and washing with absolute ethanol until the color of the precipitate turned white, the product was collected and recrystallized with distilled water, so the percentage of the product was (78%) and the melting point was (170C°)⁽¹¹⁾.

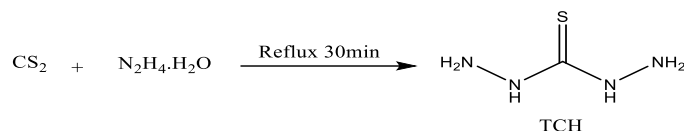


Figure (1) Preparation of thiocarbohydrazide

2.2. Preparation of reduced graphene oxide derivatives decorated with aromatic rings by the electrochemical method

ArRGO derivatives were prepared following the following steps:

First: Preparation of diazonium salts.

Dissolve 0.2g of 4-amino benzoic acid in a 100ml beaker containing an acid solution (5:5water: hydrochloric acid37%) and place it in an ice bath to maintain the temperature of the solution between (0-5C°), and in another beaker, dissolve 0.2g of 4-amino benzoic acid. 0.07g of sodium nitrite in 2ml of distilled water and added to the first solution, keeping the solution in the ice bath with continuous stirring for 30minutes in a dark atmosphere⁽¹²⁾. It was not diagnosed but was used in the next step.

Second: Preparation of sheets decorated with aromatic rings B4:Ar-RGO

Dissolve 0.1g of wheat straw reduced graphene oxide (B3:TSRGO) in 25ml of distilled water, then place it in an ultrasonic bath until it becomes clear, then add it to the electrical cell at a voltage of (2 volts) with continuous stirring, then add the solution of the first step to it. In the form of drops while remaining in the ice bath, it was left in the cell for 24 hours with continuous stirring, then it was filtered with a nanofilter, washed several times with ionic water, and dried at a temperature of 70C° until the weight was stable, so the percentage of the product was (81%)⁽¹³⁾

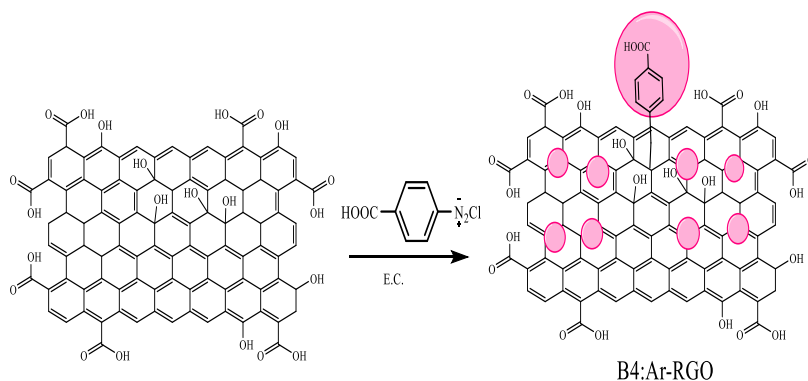


Figure (2) Preparation of the compound (B4:Ar-RGO)

2.3. Preparation of ArRGO derivatives containing 4-amino-1,2,4-triazole (B5)

Mix 0.1g of (B4:Ar-RGO) with 0.4g of thiocarbohydrazide in a heat-resistant beaker, then heat the mixture at a temperature of 170 C° while stirring with a glass stirrer. Until the color and consistency change, the result is cooled and treated with a 10% solution of sodium bicarbonate to get rid of it. Of the remaining unreacted acid, it was then filtered and dried at 60C°, and the percentage of the product was (64%).⁽¹⁴⁾

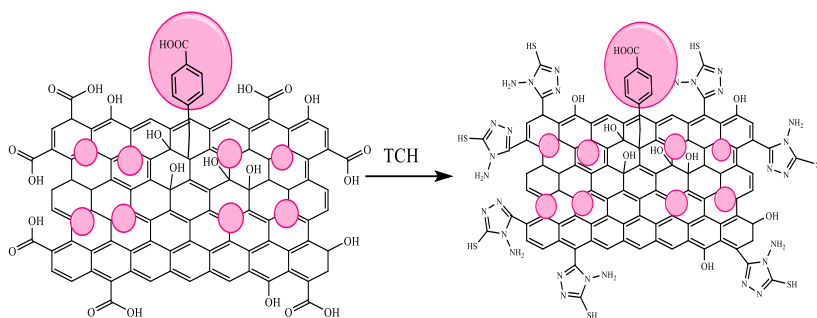


Figure (3) Preparation of compound (B5)

2.4. Preparation of 4-amino-1,2,4-triazole reduced graphene oxide - Schiff base (B7, B8)

Dissolve 0.1g of suitable aldehyde (2-hydroxybenzaldehyde and benzaldehyde) in a round flask, then add 5ml of absolute ethanol to it, add 3drops of glacial acetic acid, and add to it a solution consisting of dissolving 0.1g of ortho-amino-reduced graphene oxide (B5) in 5ml of absolute ethanol, and the system was heated for 3hours at 70C° (15)

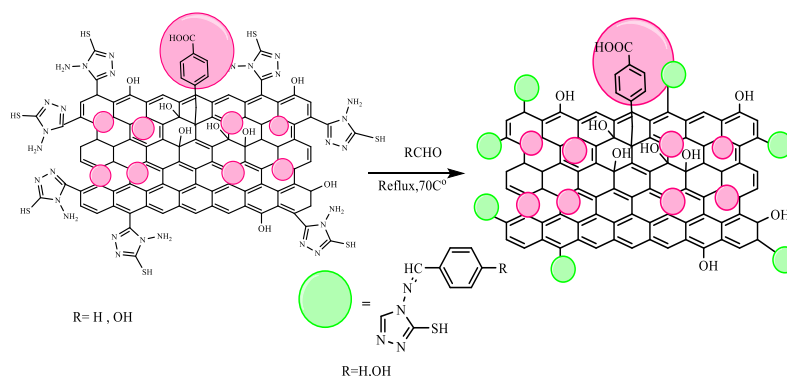
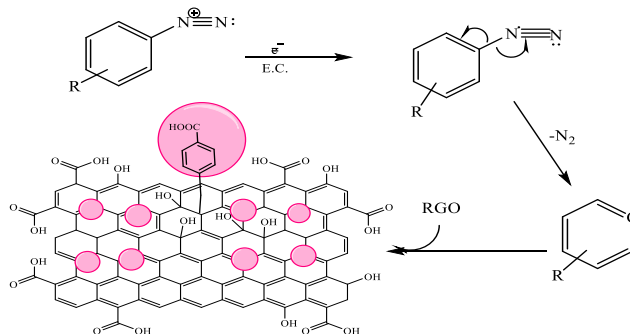


Figure (4) Preparation of compounds (B8, B7)

3. Results and discussion:

3.1. Discussion of sheets decorated with aromatic rings B4:Ar-RGO

Highly aromatic nano-reduced graphene was electrochemically decorated using 4-amino benzoic acid, which was added to it in an acidic medium, and sodium nitrite was added to it, with the presence of the prepared reduced graphene oxide (B3:TSRGO) in an aqueous medium under the influence of sound waves (Ultrasonic), then a differential was applied. The voltage in the electrical cell is below a difference of (2V), where the process of oxidation and reduction occurs in the mixture in the presence of the diazonium salt formed, according to the mechanics in diagram (1) (16).



Scheme (1) of the proposed mechanism for preparing the compound B4:Ar-RGO

When studying the infrared (IR) spectrum of sheets decorated with aromatic rings (B4), an absorption band appeared at $(3398)\text{cm}^{-1}$ belonging to the alcoholic(OH) bond of the ring, and a broad band appeared at $(3070)\text{cm}^{-1}$ dating back to the stretching of the(OH) bond. OH) carboxylate, and the

appearance of an absorption band at $(1685) \text{ cm}^{-1}$ belonging to the carboxyl ($\text{C}=\text{O}$) carbonyl bond, and the appearance of two absorption bands at $(1593, 1489) \text{ cm}^{-1}$ belonging to the aromatic ($\text{C}=\text{C}$) bond, and an absorption band also appeared At $(1319) \text{ cm}^{-1}$, it returns to the ($\text{C}-\text{O}$) bond, as shown in Figure (5), and the diagnostic packages were close to what is found in the literature ⁽¹⁷⁾.

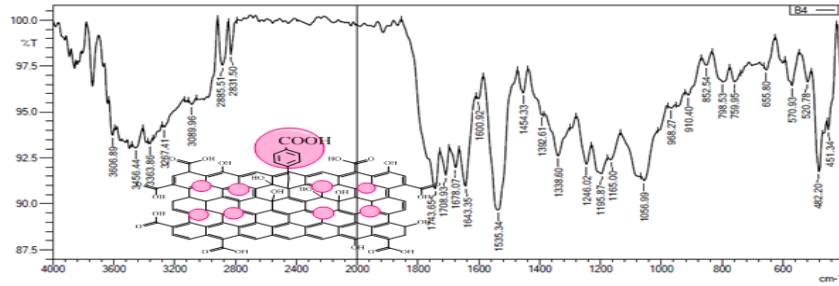


Figure (5) IR spectrum of compound B4:Ar-RGO

As for the X-ray spectrum of the compound (B4:Ar-RGO), it showed an angle value of $2\theta=45.363$, the distance between the layers $d=1.998$, the grain size $D=32.639$, and the number of layers $n=13.535$, as in Figure (6).

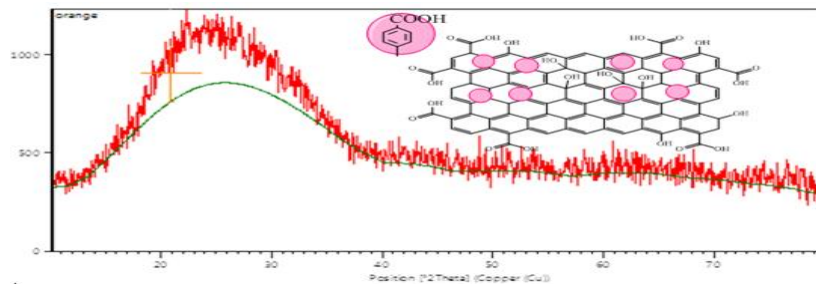


Figure (6) X-ray spectrum of compound B4:Ar-RGO

From observing the morphological images of the compound (B4:Ar-RGO) in Figure (7) using a scanning electron microscope (FESEM), there are good surface spacing of the sample with the presence of small aggregates of up to 9.04 nm that are homogeneously spread. This may indicate the wide possibility of ion decoration occurring. Carbonium resulting from diazonium salts (A), the presence of deep grooves between the plates (B), and the clarity of the zigzags and spacing of the layers explains the high surface area of the sample (C), and the presence of more aggregates at the edges with the presence of some cracks not surrounded by the aggregates, which indicates the occurrence of cracking after the completion of The decorating process, and this indicates that the time required for the decoration to occur is less than the time used (D).

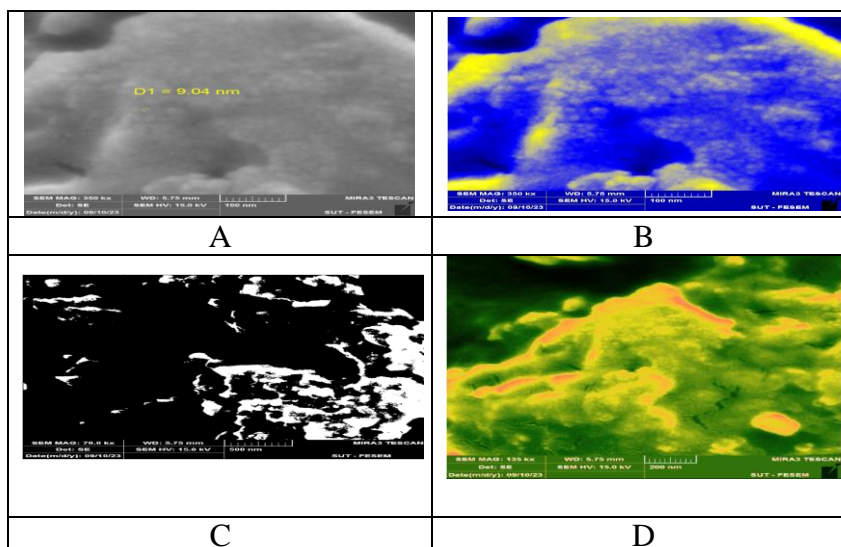


Figure (7) FESEM scanning electron microscope images of the compound B4:Ar-RGO

The transmission electron microscope (TEM) images of the compound (B4:Ar-RGO), as shown in Figure (8), showed the presence of clear peeling on the edges of the large plates. The peeling is in the form of spaced circles, which is similar to the image of a hurricane on the beach (A), and the presence of clear multilayering resulting from the peeling. (B), and the presence of cracks on the surface of the wide plates, in close areas, in a pink shape. This indicates the presence of plates containing many cavities within the material and thus a decrease in its density. (C), and the presence of the phenomenon of nanoflowers, whose formation is attributed to the retention and then explosion of nitrogen gas from between the inner plates, forming the shape of the flower. With nanometers and transparent pink leaves (D).

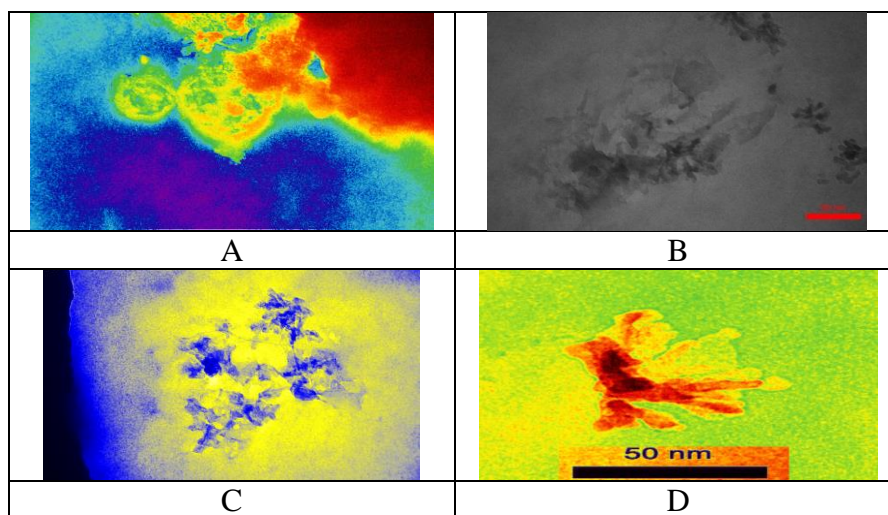


Figure (8) TEM images of the compound B4:Ar-RGO

The morphological images (AFM) by atomic force microscopy in Figure(9) of the compound (B4:Ar-RGO) showed the presence of longitudinal cavities along the sheet (A), the presence of clear surface pores (B) and the aggregates spread homogeneously on the surface (C). And the presence of heights on the surface of the plate reaching 80.6cm, which gives an additional area to the plate (D).

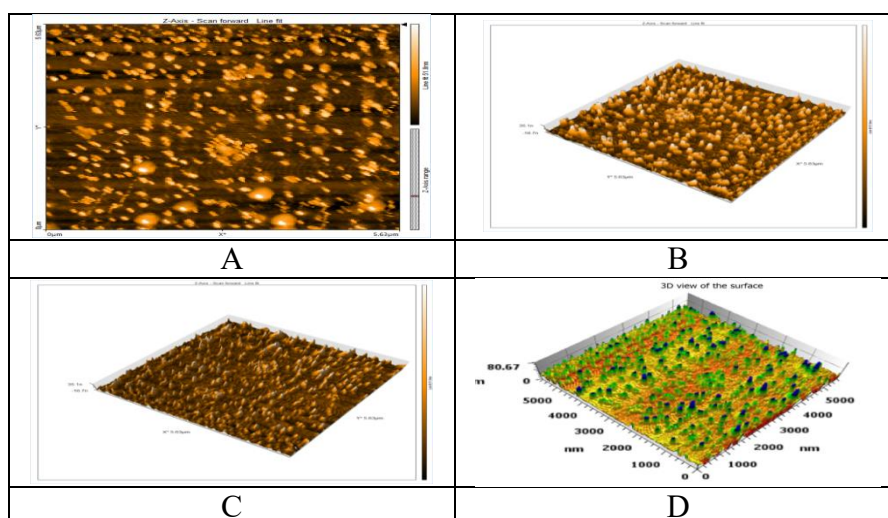
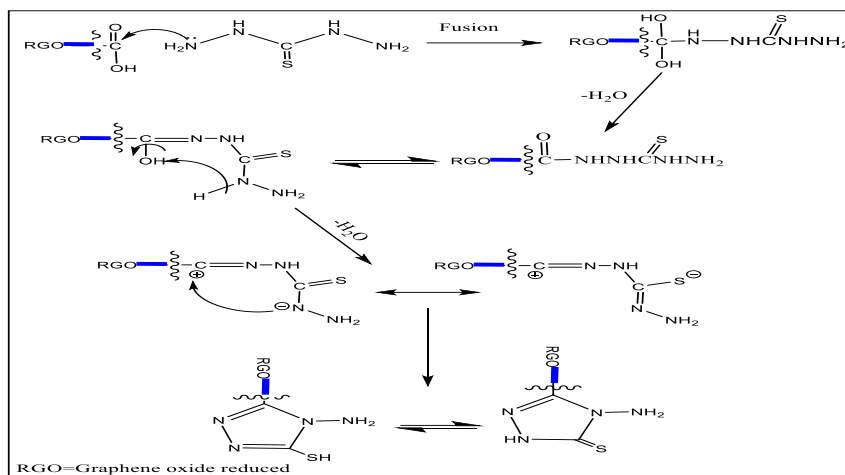


Figure (9) AFM images of the compound B4:Ar-RGO

3.2. Preparation of ArRGO derivatives containing 4-amino-4,2,1-triazole (B5)

A triazole-reduced graphene oxide composite was prepared through the thermal melting reaction of(B4:Ar-RGO) with the prepared thiocarbohydrazide (TCH) at its melting point within(1-2)minutes, and the reaction was carried out according to the mechanism suggested in the scheme(2).



Scheme (2) proposed mechanical preparation of compound (B5)

It showed a band at (1639 cm^{-1}) that belongs to the $(\text{C}=\text{N})$ bond, two bands at $(3271\text{ and }3302\text{ cm}^{-1})$ that belong to the symmetrical and asymmetric stretching of the (NH_2) group, and a band at (1284 cm^{-1}) that belongs to the (NH_2) group. $\text{C}-\text{N}$ and (2769 cm^{-1}) are due to stretching of the $(\text{S}-\text{H})$ sphincter, and the appearance of a band at (3174 cm^{-1}) of aromatic $(\text{C}-\text{H})$ stretching, and a band (3425 cm^{-1}) which is attributed to stretching of the phenolic (OH) sphincter in addition to the appearance Two bands at $(1527\text{ and }1489\text{ cm}^{-1})$ belong to the aromatic $(\text{C}=\text{C})$ sphincter stretch, as shown in Figure (10). The diagnostic bands were close to what is found in the literature (18).

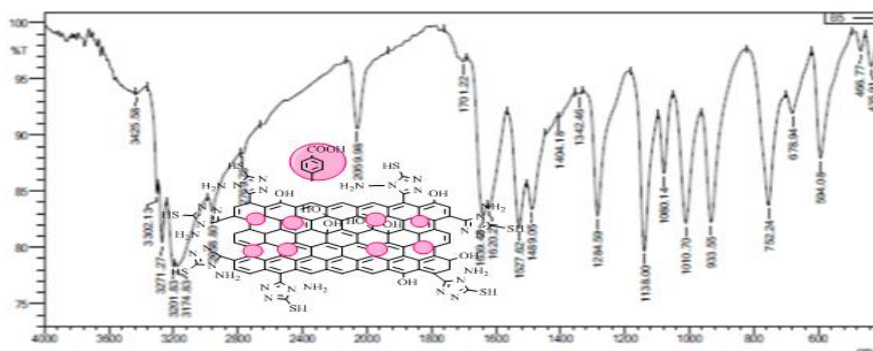


Figure (10): Infrared spectrum of compound (B5)

The X-ray spectrum of compound (B5) showed an angle value of $2\Theta=27.962$ at, the distance between the layers $d=3.188$, the grain size $D=42.507$, and the number of layers $n=3.338$, as in Figure(11).

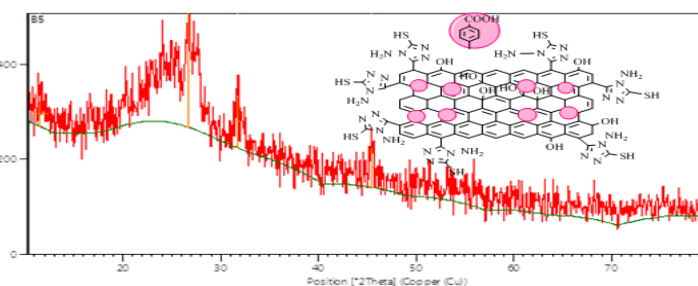


Figure (11) X-ray spectrum of compound (B5)

From observing the morphological images of compound (B5) in Figure (12) using a scanning electron microscope (FESEM), it was observed that there is a clear thickening with clusters occurring on the edges and surface of the plate, with an increase in the particle size to $(44.851)\text{nm}$. This is attributed to the ability of the triazole ring to bind the layers. And the formation of hydrogen bonds, and this is supported by the surface area value of $9.16\text{ m}^2/\text{g}$, which is one of the lowest values of surface area measurements for the prepared samples (A), the formation of a smooth layer of layered aggregate over

the carbon sheets, and this also explains the decrease in the surface area of the sample (B), and the presence of clear grooves, and this indicates To the aggregation of the plates and the occurrence of gaps and defects in the sample (C), the appearance of a spread of aggregates on some surfaces, and this indicates an increase in the amount of TCH added (D).

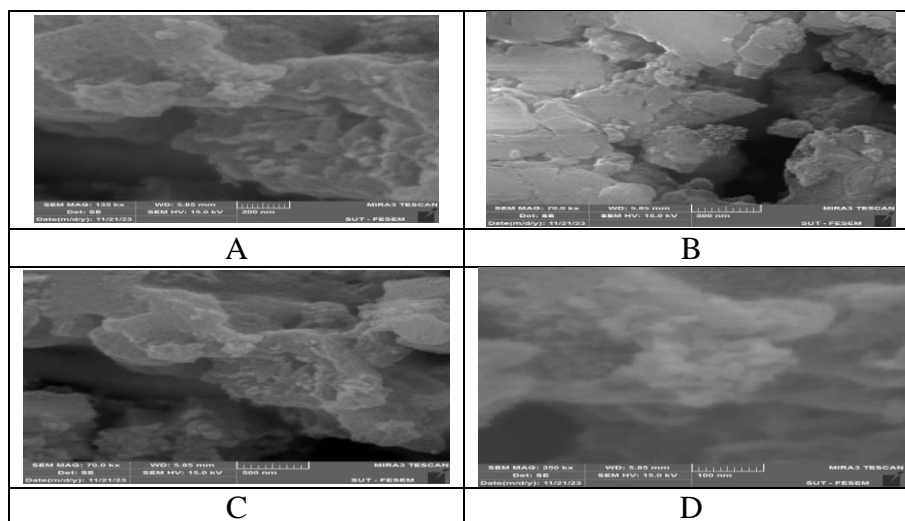


Figure (12): FESEM scanning electron microscope images of compound (B5)

Transmission electron microscope (TEM) images of compound (B5), as shown in Figure (13), showed good peeling of the sheets despite the low surface area, which indicates that it is a material not suitable for gas storage. This may also be attributed to its high ability to capture and retain gases or elements, and this is what was observed when hunting. Heavy elements (A), the presence of transparent sheets and areas with few defects. This is due to the occurrence of heterogeneous peeling of the sample and indicates the need for additional peeling electrically and not chemically (B), the presence of pink structures indicating the occurrence of the phenomenon of gas explosion with local transparent peeling with the appearance of defects in Layers (C), the presence of granular aggregates attributed to the increased amount of added TCH (D).

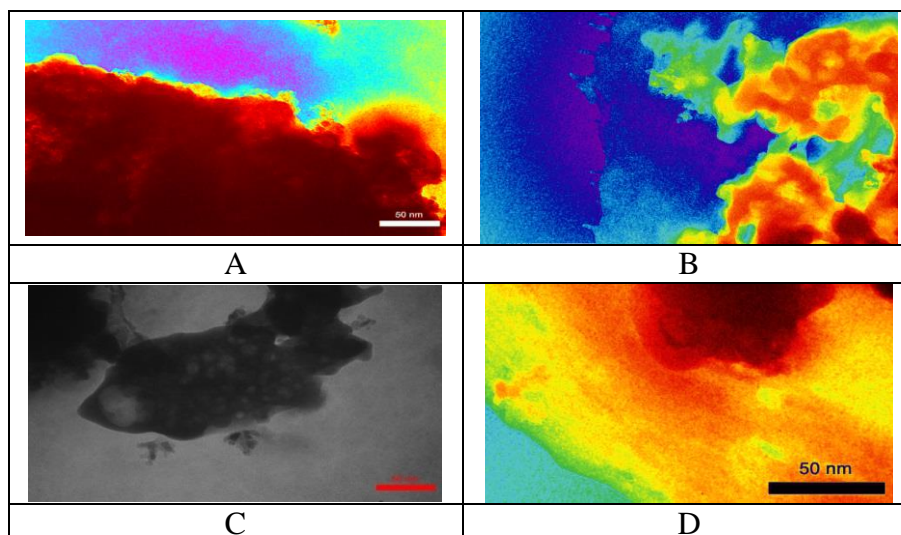


Figure (13): Transmission electron microscope (TEM) images of compound (B5)

The morphological images (AFM) using the atomic force microscope in Figure (14) of compound (B5) showed the appearance of the spread of decorations on the surface of the sheets, and this is proportional to the decrease in the surface area to $9.16 \text{ m}^2/\text{g}$, and this is attributed to the increase in the polarity of the sheets due to the aggregation of TCH molecules. And the formation of triazoles on the edges, which increases the ability of the plates to bond, increases the grain size, and reduces the surface area due to reducing the gaps between the plates (A), the presence of aggregates on the surface

due to the formation of triazole rings (B), and the appearance of the edges of the plates being very thick (C). , There is no consistent pattern of diffusion on the surface (D).

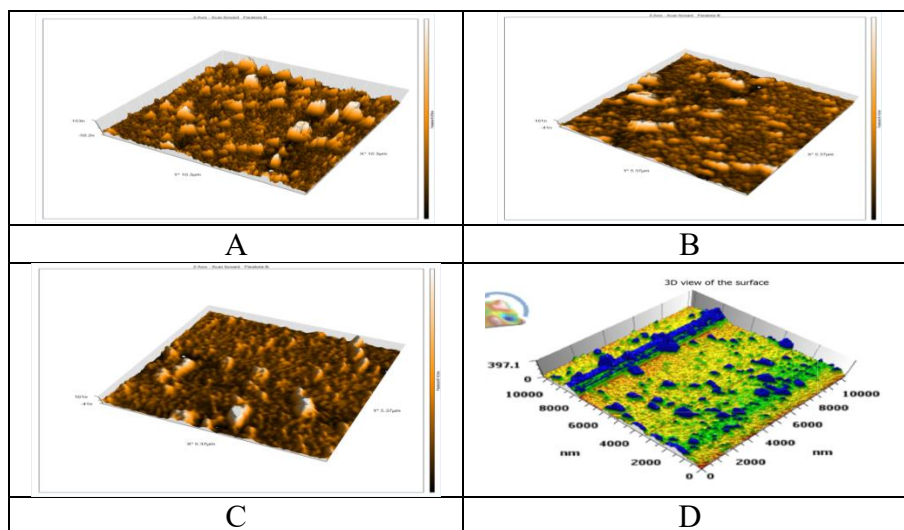
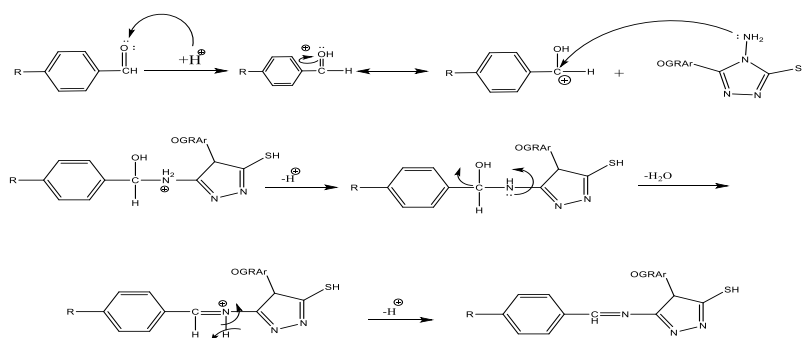


Figure (14) AFM images of compound (B5)

3.3. Discussion of the compound decorated with ortho-aminobenzoic RGO-Schiff bases(B7,B8)

A Schiff base adsorbent was prepared by reacting ortho-aminobenzoic-reduced graphene oxide with (2- bromobenzaldehyde and 2-nitrobenzaldehyde), in the presence of ethanol as a solvent according to the mechanism suggested in the scheme (4).



Scheme (4) proposed mechanical preparation of compound (B7, B8)

When studying the FT-IR spectrum, an absorption band appeared at $(3477) \text{ cm}^{-1}$ belonging to the alcohol (OH) bond, in addition to the appearance of a band at $(1622) \text{ cm}^{-1}$ attributed to the stretching of the imine group ($\text{C}=\text{N}$), with the appearance The two bands of the aromatic ring were at $(1508$ and $1622) \text{ cm}^{-1}$ and were due to the stretching of the aromatic ($\text{C}=\text{C}$) bond. An absorption band also appeared at $(1286) \text{ cm}^{-1}$ and were due to the ($\text{C}-\text{N}$) bond. The bands were close to what is found in the literature ⁽¹⁹⁾.

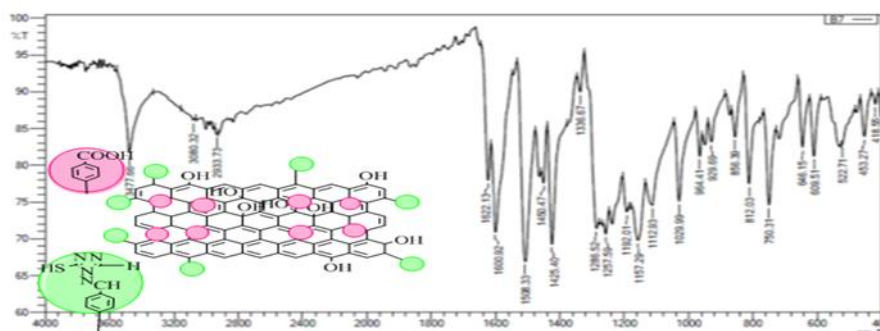


Figure (15): Infrared spectrum of compound (B7)

As for the X-ray spectrum of compound (B7), it showed an angle value of $2\theta = 22.043$ at, the distance between the layers was $d = 4.029$, the particle size was $D = 54.835$, and the number of layers was $n = 12.703$, as in Figure (16).

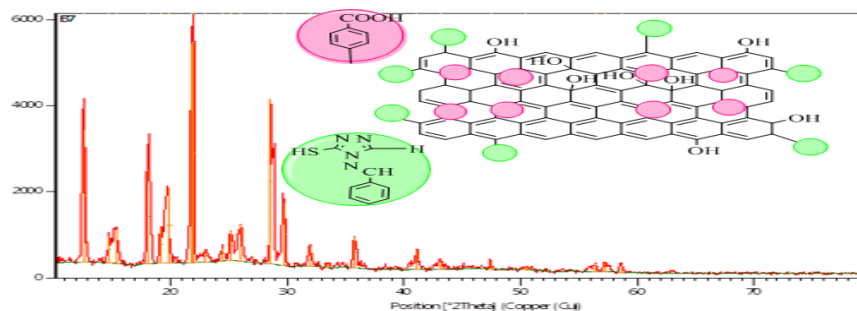


Figure (16) X-ray spectrum of compound (B7)

From observing the morphological images of compound (B7) in Figure (17) using a scanning electron microscope (FESEM), it was observed that the layered aggregation ability of the material is clear due to the presence of Schiff bases that increase the aromatic character and the ability to compact, and this explains the increase in the particle size to 57.85 nm (A). The interlocking of the layers led to the partial disappearance of defects on the plates (B), the presence of thickenings on the edges and surfaces and in the edges more clearly (C), and the presence of zigzags and twists on the surface of the plate (D)

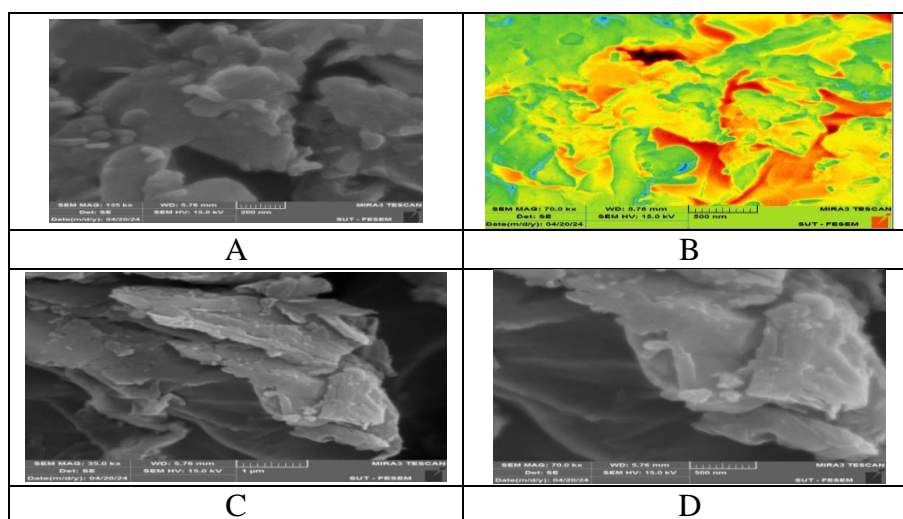


Figure (17): FESEM scanning electron microscope images of compound (B7)

Transmission electron microscope (TEM) images of compound (B7), as shown in Figure (18), showed the appearance of parchment pattern on the edges of the plates (A), and the presence of excellent peeling despite the decrease in surface area. This indicates a reduction in defects and the interconnection or overlapping of the plates (B). The presence of thickenings on the edges of the plates (C), and the presence of opposite wraps in the layers. This may explain the decrease in surface area due to the wrapping of the surface inside the formed tubes (D).

The morphological images (AFM) in Figure (19) of compound (B7) showed the presence of sharp protrusions spread over the surface (A), and the appearance of large clusters on the edges as well as on the surface, which indicates decoration clusters, and this is proportional to the grain size, which has increased significantly. Compared to B6, it reached 57.85 nm and the surface area decreased to 8.739 g/m². This is due to the increased polarity of the plates due to the polarized groups of imines, which increases the ability of the plates to bond, reduces the distance between the layers, and reduces the surface area due to reducing the gaps between the plates (B), Reduced defects on the surface of the sheets (C), and the appearance of the decoration spreading almost homogeneously on the surface (D)

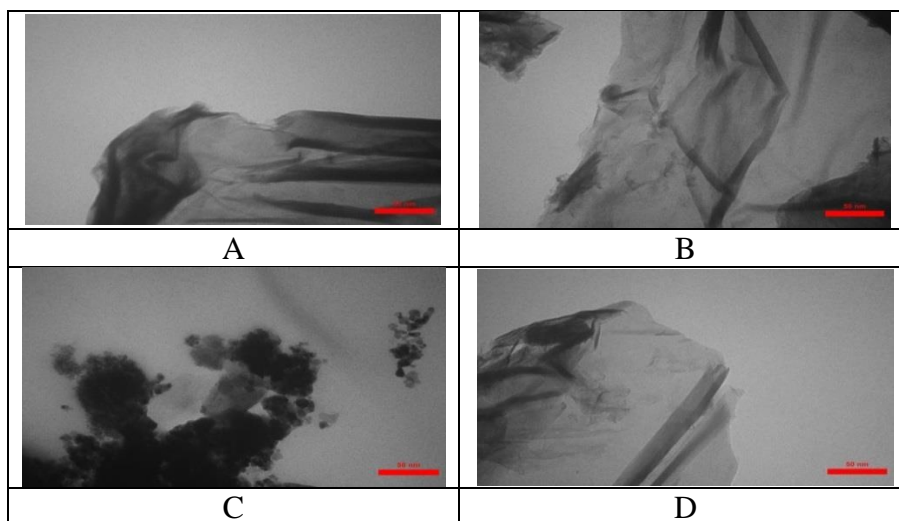


Figure (18): Transmission electron microscope (TEM) images of compound (B7)

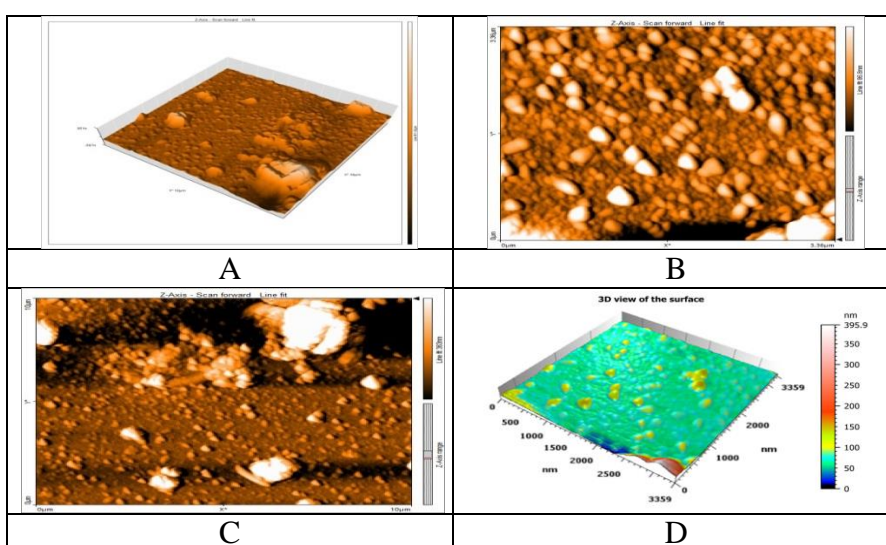


Figure (19): AFM images of compound (B7)

When studying the infrared (IR) spectrum of compound (B8), a broad absorption band appeared at $(3441) \text{ cm}^{-1}$ belonging to the phenolic (OH) bond, in addition to the appearance of a band at $(1647) \text{ cm}^{-1}$ attributed to the stretching of the imine group (C=N), with the appearance of two aromatic ring bands at $(1514 \text{ and } 1539) \text{ cm}^{-1}$ and are due to the stretching of the aromatic (C=C) bond, and an absorption band appeared at $(1338) \text{ cm}^{-1}$ dating back to the (C-N) bond, as shown in the figure (20).

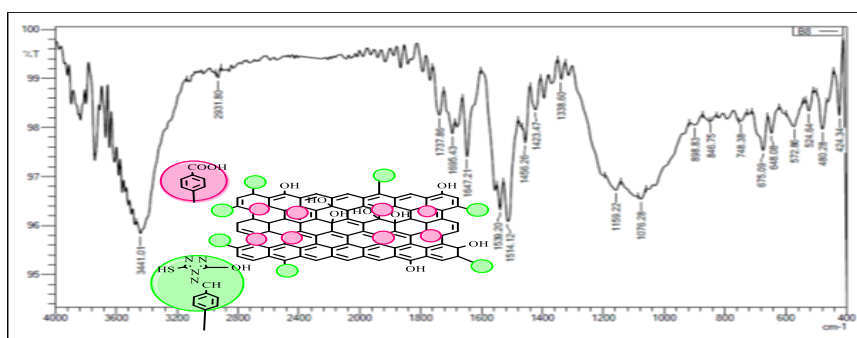


Figure (20): Infrared spectrum of compound (B8)

As for the X-ray spectrum of compound (B8), it showed an angle value of $2\theta = 31.767$ at, the distance between the layers $d = 2.815$, the grain size $D = 27.979$, and the number of layers $n = 0.364$, as in Figure (21).

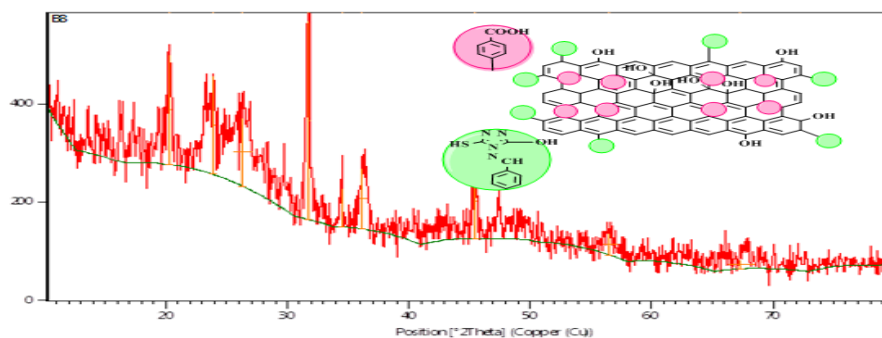


Figure (21) X-ray spectrum of compound (B8)

From observing the morphological images of compound (B8) in Figure (22) using a scanning electron microscope (FESEM), it was noted that there is a high thickening on the edges of the plates. This may be attributed to the additional hydroxy group compared to compound B7, as it increases the chances of aggregation (A). There is less peeling in the sample. Compared to B7, however, the grain size was smaller, and this may be due to the increase in the acidic character of the sample and the increase in its solubility in the solvent due to the hydroxy group of the phenolic structure (B). No curls appeared on the rims clearly (C), with the decoration spreading more homogeneously along the rims compared to With sample B7(D).

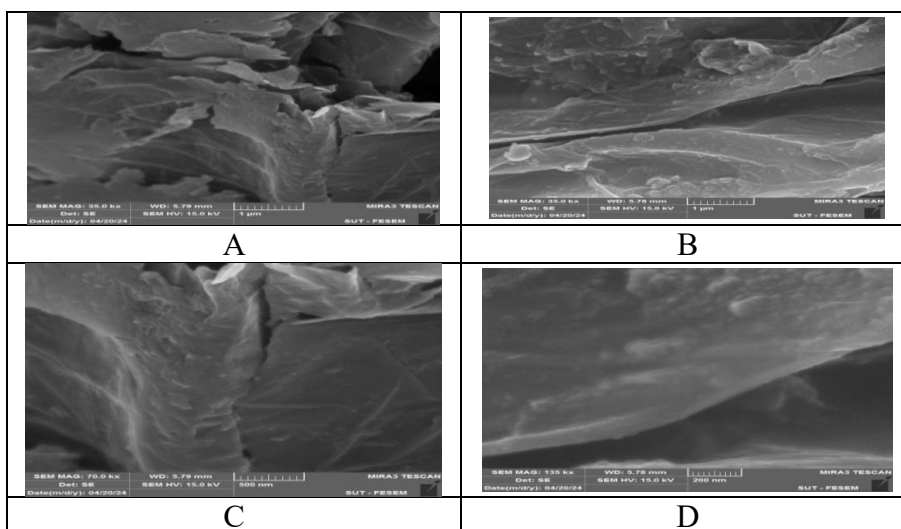


Figure (22): FESEM scanning electron microscope images of compound (B8)

The transmission electron microscope (TEM) images of the compound (B8), as shown in Figure (23), showed the appearance of large, clear gaps(A), the appearance of the supporting material on the surface of the plates and their edges (B), and the appearance of less peeling of the sample compared to B7(C). There is a less twisted fold on the surface of the sheet compared to B7(D).

The morphological images (AFM) by atomic force microscopy in Figure (24) of compound (B8) showed the spread of the decoration on the edges of the protruding sheets in Figure (A), the presence of longitudinal cavities carrying the decoration in different groups (B), and the appearance of parallel layered grouping of the material (C), difference in the height of the clusters, reaching a height of 207.5 nm (D)

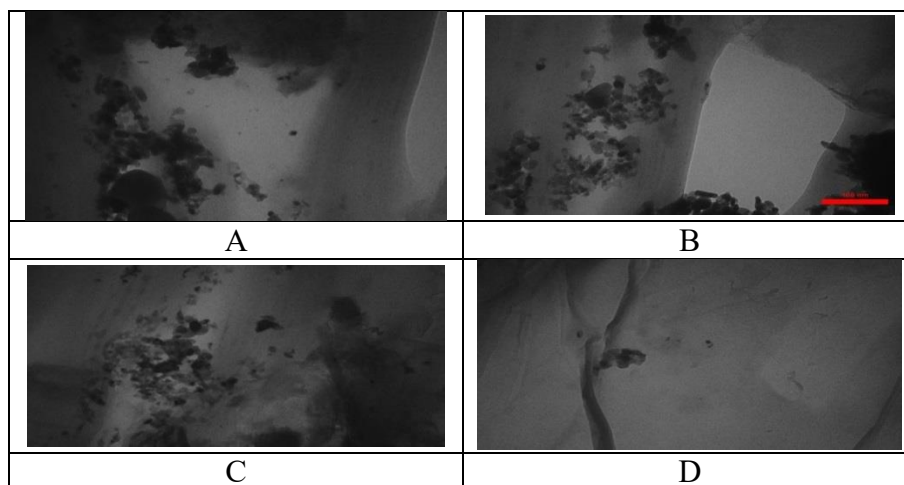


Figure (23): Transmission electron microscope (TEM) images of compound (B8)

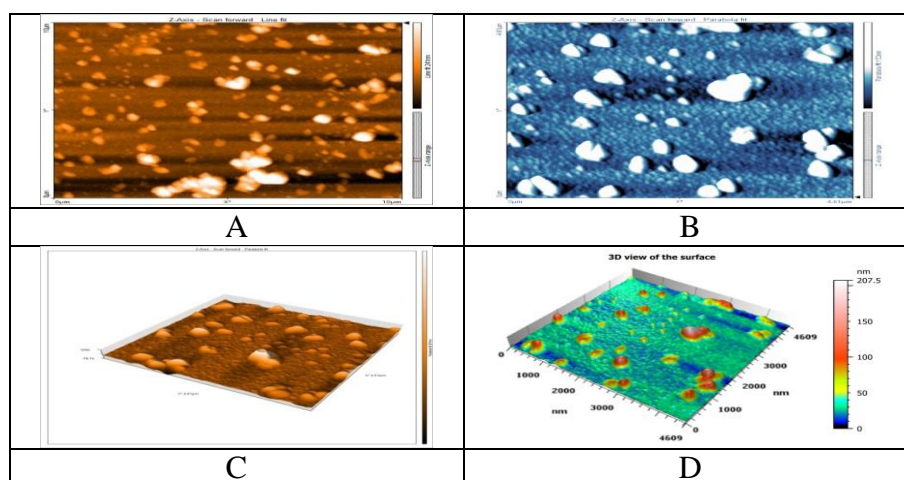


Figure (24) AFM images of compound (B8)

4. Conclusion

It was possible to decorate the highly aromatic nano-reduced graphene oxide (B4) using 4-amino benzoic acid and increase the surface area to reach $1229 \text{ m}^2/\text{g}$. Obtaining derivatives of nano-triazole reduced graphene oxide (B5) by means of thermal melting without affecting the nature of the plate bearing the decoration. It was possible to prepare a compound of Azo - reduced grapheme oxide (B6) by electrophoresis. It was possible to prepare triazole schiff bases (B7 and B8) on the edges of the nanosheets. The highest particle size was for compound B7(57.858 nm), which represents decoration by the Schiff base, and this indicates the ability of the Schiff base to increase the accumulation of reduced graphene oxide layers. The lowest value of the particle size was for the sample (B6) is (2.956 nm), which is a reduced graphene oxide azo, due to the effect of the azo bond, which changes the nature of the formation of hydrogen bonds between the amino groups on the heterogeneous ring.

References

1. Chua, C. K., & Pumera, M. (2014). Chemical reduction of graphene oxide: a synthetic chemistry viewpoint. *Chemical Society Reviews*, *43*(1), 291-312.
2. Stankovich, S., Dikin, D. A., Piner, R. D., Kohlhaas, K. A., Kleinhammes, A., Jia, Y., & Ruoff, R. S. (2007). Synthesis of graphene-based nanosheets via chemical reduction of exfoliated graphite oxide. *carbon*, *45*(7), 1558-1565.
3. Vlocskó, R. B., Xie, G., & Török, B. (2023). Green Synthesis of Aromatic Nitrogen-Containing Heterocycles by Catalytic and Non-Traditional Activation Methods. *Molecules*, *28*(10), 4153.

4. Morais, P. A., Francisco, C. S., de Paula, H., Ribeiro, R., Eloy, M. A., Javarini, C. L., ... & Júnior, V. L. (2021). Semisynthetic Triazoles as an Approach in the Discovery of Novel Lead Compounds. *Current Organic Chemistry*, 25(10), 1097-1179.
5. Gao, F., Wang, T., Xiao, J., & Huang, G. (2019). Antibacterial activity study of 1, 2, 4-triazole derivatives. *European journal of medicinal chemistry*, 173, 274-281.
6. Narsimha, S., Kumar, N. S., Swamy, B. K., Reddy, N. V., Hussain, S. A., & Rao, M. S. (2016). Indole-2-carboxylic acid derived mono and bis 1, 4-disubstituted 1, 2, 3-triazoles: Synthesis, characterization and evaluation of anticancer, antibacterial, and DNA-cleavage activities. *Bioorganic & medicinal chemistry letters*, 26(6), 1639-1644.
7. Faridbod, F., Ganjali, M. R., Dinarvand, R., Norouzi, P., & Riahi, S. (2008). Schiff's bases and crown ethers as supramolecular sensing materials in the construction of potentiometric membrane sensors. *Sensors*, 8(3), 1645-1703.
8. G. W. Wilkinson, R. D. Gillard and J. A. Mc. Cleverly, (1987), "Comprehensive Coordination Chemistry" .1st.ed., Pergamon press ,Oxford , England ,715-735.
9. A. E. Sadigova, A. M. Magerramov and A. Allakhvarder,(2003), " Preparation and diagnosis of oral rules and their derivatives derived from 4-aminuantepirin and used in the extraction of ion-nickel duo"Russian J. Genral Chem.," 73, 1932-1935.
10. M. Kobayashi, M. Yoshida and H. Minato, (1976),"Configuration of photoisomers of benzylidene-anilines", J. Org. Chem., 41. 3322.
11. Mahmood, H. G. A., Al-Sumaida, G. H. A. W., & Hamdi, A. Q. (2022). Preparation and diagnosis of nanographene oxide and nanographene oxide derivatives. *Journal of Education and Scientific Studies*, 2(20).
12. Ahmed Mohammed, A., & Abdulwahhab, G. H. (2022). Spectrophotometric Determination of Loratadine drug by New 6-hydrazineyl-3-(pyridiin-4-yl)-[1, 2, 4] triazolo [3, 4-b][1, 3, 4] thiadiazole A1 derived from isonicotinic acid in pure and pharmaceuticals formulation. *Egyptian Journal of Chemistry*, 65(132), 273-280.
13. Al-Dulaimi, A. F., Al-Somaidaie, G. H., & Jumaa'h, M. M. (2022). Electrochemical preparation of new graphene nanosheet derivatives for using in different applications. *Materials Today: Proceedings*, 49, 3538-3548.
14. Afrah, H, Hazzaa., Al-Somaidaie, G. H., & Salih, N. A. (2022). Electrochemical synthesis and characterization of aromatic decorated graphene nanosheet and reduced graphene nanosheet. *Materials Today: Proceedings*, 57, 505-514.
15. Gupta, A., & Saha, S. K. (2012). Emerging photoluminescence in azo-pyridine intercalated graphene oxide layers. *Nanoscale*, 4(20), 6562-6567.
16. Sibirian, R., Sihotang, H., Raja, S. L., Supeno, M., & Simanjuntak, C. (2018). New route to synthesise of graphene nano sheets. *Oriental Journal of Chemistry*, 34(1), 182.
17. Sarath, P. S., Moni, G., George, J. J., Haponiuk, J. T., Thomas, S., & George, S. C. (2021). A study on the influence of reduced graphene oxide on the mechanical, dynamic mechanical and tribological properties of silicone rubber nanocomposites. *Journal of Composite Materials*, 55(15), 2011-2024.
18. Sanhueza, I. A., Klauck, F. J., Senol, E., Keaveney, S. T., Sperger, T., & Schoenebeck, F. (2021). Base-Free Cross-Couplings of Aryl Diazonium Salts in Methanol: PdII-Alkoxy as Reactivity-controlling Intermediate. *Angewandte Chemie International Edition*, 60(13), 7007-7012.
19. Theophile, T. (Ed.). (2012). *Infrared spectroscopy: Materials science, engineering and technology*. BoD-Books on Demand.